

See discussions, stats, and author profiles for this publication at: <https://www.researchgate.net/publication/224124500>

Time-dependent regulation of yeast glycolysis upon nitrogen starvation depends on cell history

Article in IET Systems Biology · April 2010

DOI: 10.1049/iet-syb.2009.0025 · Source: IEEE Xplore

CITATIONS

22

READS

124

8 authors, including:



Karen van Eunen

University of Groningen

81 PUBLICATIONS **1,344** CITATIONS

[SEE PROFILE](#)



Jildau Bouwman

TNO

79 PUBLICATIONS **1,510** CITATIONS

[SEE PROFILE](#)



Walter van Gulik

Delft University of Technology

137 PUBLICATIONS **5,151** CITATIONS

[SEE PROFILE](#)



Hans V Westerhoff

The University of Manchester and University of Amsterdam and VU ...

568 PUBLICATIONS **22,113** CITATIONS

[SEE PROFILE](#)

Some of the authors of this publication are also working on these related projects:



EuroDISH: studying the need for food and health research infrastructure in Europe [View project](#)



SysMO MOSES: Microorganism Systems Biology: energy and *Saccharomyces cerevisiae* [View project](#)

Published in IET Systems Biology
 Received on 14th April 2009
 Revised on 26th August 2009
 doi: 10.1049/iet-syb.2009.0025



Time-dependent regulation of yeast glycolysis upon nitrogen starvation depends on cell history

K. van Eunen^{1,*} P. Dool¹ A.B. Canelas² J. Kiewiet¹
 J. Bouwman^{1,†} W.M. van Gulik² H.V. Westerhoff^{1,3}
 B.M. Bakker^{1,4}

¹Department of Molecular Cell Physiology, Vrije Universiteit Amsterdam, De Boelelaan 1085, 1081 HV Amsterdam, The Netherlands

²Department of Biotechnology, Delft University of Technology, Julianalaan 67, 2628 BC Delft, The Netherlands

³Manchester Centre for Integrative Systems Biology, Manchester Interdisciplinary BioCentre, The University of Manchester, 131 Princess Street, M1 7ND Manchester, UK

⁴Department of Pediatrics, Center for Liver, Digestive and Metabolic Diseases, University Medical Center Groningen, University of Groningen, Hanzeplein 1, NL-9713 GZ Groningen, The Netherlands

*Department of Chemical and Biological Engineering, Chalmers University of Technology, SE-412 96 Göteborg, Sweden

†Physiological Genomics, TNO Quality of Life, Utrechtseweg 48, 3704 HE Zeist, The Netherlands

E-mail: b.m.bakker@med.umcg.nl

Abstract: In this study, the authors investigated how the glycolytic flux was regulated in time upon nitrogen starvation of cells with different growth histories. We have compared cells grown in glucose-limited chemostat cultures under respiratory conditions (low dilution rate of 0.1/h) to cells grown under respirofermentative conditions (high dilution rate of 0.35/h). The fermentative capacity was lower in cells grown under respiratory conditions than in cells grown under respirofermentative conditions, yet more resilient to prolonged nitrogen starvation. The time profiles revealed that the fermentative capacity even increased in cells grown under respiratory conditions during the first hours of nitrogen starvation. In cells grown under respirofermentative conditions the fermentative capacity decreased from the onset of nitrogen starvation. We have applied time-dependent Regulation Analysis to follow the fermentative capacity during nitrogen starvation. In both experiments, diverse categories of regulation were found. However, in the cells grown under respiratory conditions regulation was predominantly metabolic, whereas in the cells grown under respirofermentative conditions hierarchical regulation was dominant. To study the metabolic regulation, concentrations of intracellular metabolites, including allosteric regulators, were measured. The obtained results can explain some aspects of the metabolic regulation, but not all.

1 Introduction

In *Saccharomyces cerevisiae*, high sugar concentrations and high specific growth rates ($\mu > 0.30/h$) trigger alcoholic fermentation, even under fully aerobic conditions. This so-called respirofermentative growth results in a lower biomass

yield, but a higher fermentative capacity than fully respiratory growth [1]. The fermentative capacity is defined as the specific rate of carbon dioxide (and ethanol) production immediately upon introduction of the yeast into an anaerobic glucose-excess environment such as during the leavening of dough. Several studies showed a more stable

fermentative capacity when cells were grown under conditions that favour respiratory growth and were subsequently subjected to for instance cold or nutrient stress [2, 3]. Similarly, a *hxx2Δ* mutant strain, which shows almost fully respiratory growth even at high glucose concentrations [4], has a more stable fermentative capacity [5]. In general, this suggests an inverse correlation between glucose repression and the resilience of fermentative capacity towards stress [5].

Rossell *et al.* [5] started investigating how this relation between glucose repression and the stability of fermentative capacity was regulated at the levels of enzyme expression and metabolism. They found that in the *hxx2Δ* mutant, but not in the wild type, the activities of the glycolytic enzymes were stable or even increased after 24 h of nitrogen starvation. Here we will analyse the dependence of the stability of the fermentative capacity upon the history of the cells in more depth by following regulation of the fermentative capacity in time. To this end we will use an extension of Regulation Analysis [6, 7] in which regulation coefficients are quantified as a function of time [8]. Time-dependent Regulation Analysis unravels quantitatively and dynamically how functional changes in the cell are brought about by the interplay of gene expression (hierarchical regulation) and metabolism (metabolic regulation).

The original form of Regulation Analysis has been developed to compare two steady states. An elaborate description of Regulation Analysis can be found in Rossell *et al.* [6, 9]. Briefly, the method can dissect gene-expression and metabolic regulation applying the following equation as derived previously [6, 7, 9]

$$1 = \frac{\Delta \log V_{\max,i}}{\Delta \log J_i} + \frac{\Delta \log g_i(X, K)}{\Delta \log J_i} = \rho_{h,i} + \rho_{m,i} \quad (1)$$

Here, J denotes the flux through enzyme i . Δ denotes the difference between two steady states. The hierarchical regulation coefficient ρ_h quantifies the relative contribution of changes in capacity of enzyme i ($V_{\max,i}$) to the regulation of the flux through enzyme i . The hierarchical regulation coefficient is associated with changes in the entire gene expression cascade all the way from transcription to protein synthesis, stability and modification. The relative contribution of changes in the interaction of the enzyme with the rest of metabolism is reflected in the metabolic regulation coefficient ρ_m . Changes in the metabolic function g are caused by changes in concentrations of substrates, products and effectors (X), and by changes in affinities (K) of enzyme i towards its substrates, products and effectors. And, together the two regulation coefficients should describe regulation completely, that is add up to 1. Experimentally, the hierarchical regulation coefficient is the one that is more readily determined, as it requires only measurements of the V_{\max} of enzyme i and the flux through

it under two conditions, according to

$$\rho_{h,i} = \frac{\Delta \log V_{\max,i}}{\Delta \log J_i} \quad (2)$$

The metabolic regulation coefficient can then be calculated from the summation law ($\rho_m = 1 - \rho_h$).

The time-dependent extension of Regulation Analysis quantifies the regulation coefficients as a function of time [8]. For this study we have used the integrative version of time-dependent Regulation Analysis, which integrates all the changes between time point t_0 (the start of the perturbation) and time point t . This results in the following equations

$$\rho_{h,i}(t) = \frac{\log V_{\max,i}(t) - \log V_{\max,i}(t_0)}{\log J_i(t) - \log J_i(t_0)} \quad (3)$$

$$1 = \rho_{h,i}(t) + \rho_{m,i}(t) \quad (4)$$

in which $\rho_{h,i}$ and $\rho_{m,i}$ are the hierarchical and metabolic regulation coefficients of enzyme i , respectively, $V_{\max,i}$ is the catalytic capacity of enzyme i and J_i is the in vivo flux through enzyme i . For a more elaborate description and discussion of the method, see Bruggeman *et al.* [8].

The aim of the present study is to understand how the regulation of fermentative capacity as a function of time depends on the history of the cells. We will apply time-dependent Regulation Analysis to follow the fermentative capacity during nitrogen starvation. We will compare cells grown in aerobic glucose-limited chemostats under respiratory conditions (low dilution rate) to cells grown under respirofermentative conditions (high dilution rate [10]).

2 Material and methods

2.1 Strain and growth conditions

The haploid, prototrophic *Saccharomyces cerevisiae* strain CEN.PK113-7D (*MATa*, *MAL2-8^c*, *SUC2*) was cultivated in an aerobic, glucose-limited chemostat (1l laboratory fermentor, Applikon) as described in detail by Van Hoek *et al.* [11]. Chemostat cultures were fed with defined mineral medium [12] in which glucose (42 mM) was the growth-limiting nutrient. Yeast cells were grown under either respiratory or respirofermentative conditions at a dilution rate of 0.1 or 0.35/h, respectively.

2.2 Nitrogen-starvation experiment

For the nitrogen-starvation experiments the same defined mineral medium was used as for the chemostat culture, but it lacked ammonium sulphate and contained an excess of glucose (195 mM, see also Results section). Yeast cells harvested from steady-state chemostats were washed with ice-cold starvation medium and resuspended in starvation

medium to a dry weight concentration of approximately 2 g/l. Cells were brought back in a new fermentor in batch mode (start volume was around 1 l) at otherwise the same conditions as during chemostat cultivation. Samples were taken for measuring the fermentative capacity and the capacities of the glycolytic and fermentative enzymes. We have taken samples at time points 0, 2, 4, 8 and 24 h after the onset of starvation. After all samples had been taken, the remaining culture volume was around 500 ml.

2.3 Fermentative capacity and steady-state fluxes

The set-up used for the determination of fermentative capacity has been described by Rossell *et al.* [6]. Briefly, the fermentative capacity is measured as the rate of ethanol production in an off-line assay in which cells are transferred to a complete growth medium under anaerobic conditions at excess of glucose. Culture samples were taken and cells were washed and taken up in defined mineral medium [12] lacking glucose. The fermentative capacity and the steady-state fluxes were measured under anaerobic conditions with excess of glucose (56 mM, added at time 0) for 30 min in a 6% wet weight cell suspension at 30°C. The concentrations of ethanol, glucose, glycerol, succinate, pyruvate, acetate and trehalose were measured by high pressure liquid chromatography (HPLC) analysis (300 mm × 7.8 mm ion exchange column Aminex-HPX 87H (Bio-Rad) kept at 55°C, with 22.5 mM H₂SO₄ as eluent at a flow rate of 0.5 ml/min). The HPLC was calibrated for all the metabolites measured.

For the intracellular metabolite samples, the medium was adapted to prevent interference of high sulphate concentrations during the liquid-chromatography mass spectrometry/mass spectrometry (LC-MS/MS) run. Then the assay was carried out in medium with 2.27 mM ammonium sulphate, 26.08 mM ammonium phosphate, 2.2 mM potassium phosphate and 2.03 mM magnesium sulphate. Vitamins and trace elements were added in the same concentrations as in the minimal medium according to Verduyn *et al.* [12]. Glucose concentration was in both media 56 mM and pH was adjusted to 5.6 with KOH. The change in medium composition did not have an influence on the measured fluxes (data not shown). The fluxes through the individual enzymes were calculated from steady-state rates of the glucose consumption and the ethanol and glycerol production. Fig. 2 shows a simplified scheme of the pathway in which enzymes with the same flux are boxed together. Flux through hexokinase (HXK) is equal to glucose flux. Fluxes through phosphoglucose isomerase (PGI), phosphofructokinase (PFK) and aldolase (ALD) were calculated by dividing the sum of the glycerol and ethanol fluxes by two. The fluxes through the enzymes from glyceraldehyde-3-phosphate dehydrogenase (GAPDH) to alcohol dehydrogenase (ADH) were taken to be equal to the measured ethanol flux. Other products of glucose metabolism, that is succinate, acetate and pyruvate,

were negligible. Implicitly, it is assumed in these calculations that small gaps in the carbon balance must be attributed to branches at the level of glucose-6-phosphate (G6P), that is the pentose-phosphate pathway or the breakdown/synthesis of storage carbohydrates.

2.4 Enzyme capacity measurements

For preparation of cell-free extracts, samples were harvested, washed twice with 10 mM potassium phosphate buffer (pH 7.5) containing 2 mM Na₂H₂-EDTA, concentrated 10-fold and stored at -20°C. Samples were thawed, washed and resuspended in an equal volume of 100 mM potassium phosphate buffer (pH 7.5) containing 2 mM MgCl₂ and 1 mM dithiothreitol. Cell-free extracts were prepared freshly by using the FastPrep[®] method with acid-washed glass beads (425–600 microns, Sigma). Eight bursts of 10 s at a speed of 6.0 were done. In between the bursts, samples were cooled on ice for at least 1 min. Enzyme capacities (V_{max}) were measured by NAD(P)H-linked assays [11], using the Novostar (BMG Labtech) as an analyser for spectroscopic measurements. All enzyme assays were done at four concentrations of cell-free extracts to confirm that the reaction rates were proportional to the amounts of cell extract added. Protein concentrations were determined by using the Bicinchoninic Acid kit (Pierce) with bovine serum albumin (BSA) (2 mg/ml stock solution, Pierce, containing 1 mM dithiothreitol) as standard.

The activities of triosephosphate isomerase (TPI), phosphoglycerate mutase (GPM) and enolase (ENO) were not measured. The activity of TPI measured under the conditions described in [11] is extremely high. Since the high values of TPI activity could not be compared in a statistically sound manner, we have decided to exclude TPI activity measurements from our data set. Since some of the substrates for GPM and ENO were not supplied anymore in sufficiently pure quality, the latter two enzymes could not be measured either.

2.5 Intracellular metabolite concentrations

Samples were taken 15 min after the start of the fermentative capacity assay to the protocol described by Canelas *et al.* [13]. The exact sample weights were determined by weighing the tube before and directly after sampling. Quenching and washing of the sample was done with 100% and 80% (v/v) methanol/water, respectively, at -40°C and intracellular metabolite extraction was carried out using the boiling ethanol method [14], as described in Lange *et al.* [15]. U-¹³C-labelled cell extract was added to the pellets just before the extraction, as internal standard. Sample concentration was accomplished by evaporation under vacuum, as described by Mashego *et al.* [16]. The concentrations of the intracellular metabolites were determined by electrospray-ionisation liquid-chromatography

Table 1 Physiological parameters of the aerobic glucose-limited chemostat cultures before the nitrogen-starvation experiments

Dilution rate, h^{-1}	Yield _{glu,x} , g/g	$q_{O_2}^a$	$q_{CO_2}^b$	RQ ^c	$q_{glucose}^a$	$q_{ethanol}^b$	Dry weight, g/l	Carbon recovery, %
0.1	0.45 ± 0.02	2.8 ± 0.0	3.0 ± 0.1	1.1 ± 0.0	1.2 ± 0.0	n.d.	3.7 ± 0.1	94 ± 3
0.35	0.29 ± 0.01	7.2 ± 0.2	12.9 ± 0.4	1.8 ± 0.0	6.8 ± 0.1	5.2 ± 0.2	2.2 ± 0.1	93 ± 1

Errors represent standard error of the mean (SEM) of at least three independent chemostat cultures

^ammol consumed per gram biomass per hour

^bmmol produced per gram biomass per hour

^cRespiratory quotient (q_{CO_2}/q_{O_2}); n.d.: not detectable

mass spectrometry/mass spectrometry (ESI-LC-MS/MS) [17] and the quantification was based on isotope dilution mass spectrometry (IDMS) [16, 18]. Adenosine triphosphate (ATP), adenosine diphosphate (ADP) and adenosine monophosphate (AMP) were analysed by ion-pairing reversed-phase ESI-LC-MS/MS as described in [19].

3 Results

3.1 Fermentative capacity and steady-state fluxes

Yeast was grown in aerobic glucose-limited chemostat cultures at a dilution rate (D) of 0.1/h (respiratory) or 0.35/h (respirofermentative). Steady-state values showed indeed a

Table 2 C-flux in mmol C/min/gProtein during fermentative capacity assay

Growth rate	Metabolite	t_0	t_2	t_4	t_8	t_{24}
$D = 0.1/h$	glucose	-2.13 ± 0.10	-3.29 ± 0.39	-3.04 ± 0.22	-2.17 ± 0.37	-1.11 ± 0.22
	ethanol	1.10 ± 0.03	1.49 ± 0.15	1.56 ± 0.07	1.27 ± 0.07	0.97 ± 0.09
	glycerol	0.20 ± 0.02	0.28 ± 0.01	0.27 ± 0.00	0.24 ± 0.02	0.16 ± 0.00
	trehalose	-0.09 ± 0.01	-0.06 ± 0.03	-0.09 ± 0.03	-0.27 ± 0.06	-0.33 ± 0.01
	pyruvate	0.02 ± 0.01	0.03 ± 0.01	0.03 ± 0.00	0.02 ± 0.01	0.02 ± 0.00
	succinate	0.01 ± 0.00	0.00 ± 0.00	0.00 ± 0.00	0.00 ± 0.00	0.00 ± 0.00
	acetate	0.02 ± 0.00	0.00 ± 0.00	0.00 ± 0.00	0.00 ± 0.00	0.00 ± 0.00
	CO ₂	0.55 ± 0.01	0.74 ± 0.08	0.78 ± 0.04	0.64 ± 0.03	0.48 ± 0.05
	total consumed carbon	2.22 ± 0.11	3.35 ± 0.38	3.14 ± 0.19	2.44 ± 0.31	1.44 ± 0.37
	total produced carbon	1.90 ± 0.02	2.54 ± 0.25	2.64 ± 0.11	2.17 ± 0.12	1.63 ± 0.13
$D = 0.35/h$	glucose	-2.42 ± 0.13	-2.21 ± 0.01	-1.87 ± 0.09	-1.95 ± 0.04	-1.55 ± 0.42
	ethanol	1.28 ± 0.07	1.11 ± 0.02	1.11 ± 0.06	1.22 ± 0.05	1.04 ± 0.01
	glycerol	0.23 ± 0.01	0.25 ± 0.02	0.24 ± 0.00	0.23 ± 0.00	0.20 ± 0.02
	trehalose	0.04 ± 0.01	-0.06 ± 0.04	-0.09 ± 0.01	-0.31 ± 0.00	-0.35 ± 0.20
	pyruvate	0.02 ± 0.01	0.02 ± 0.01	0.01 ± 0.01	0.02 ± 0.00	0.02 ± 0.01
	succinate	0.01 ± 0.00	0.01 ± 0.00	0.00 ± 0.00	0.00 ± 0.00	0.00 ± 0.00
	acetate	0.02 ± 0.00	0.02 ± 0.00	0.02 ± 0.00	0.00 ± 0.00	0.01 ± 0.01
	CO ₂	0.65 ± 0.03	0.56 ± 0.01	0.56 ± 0.03	0.61 ± 0.02	0.52 ± 0.00
	total consumed carbon	2.42 ± 0.13	2.27 ± 0.05	1.96 ± 0.09	2.27 ± 0.04	1.90 ± 0.22
	total produced carbon	2.25 ± 0.10	1.97 ± 0.04	1.94 ± 0.08	2.08 ± 0.06	1.79 ± 0.03

Errors represent SEM of at least three independent experiments carried out on different chemostat cultures. Data for $D = 0.35/h$ were reproduced from [10] for comparison

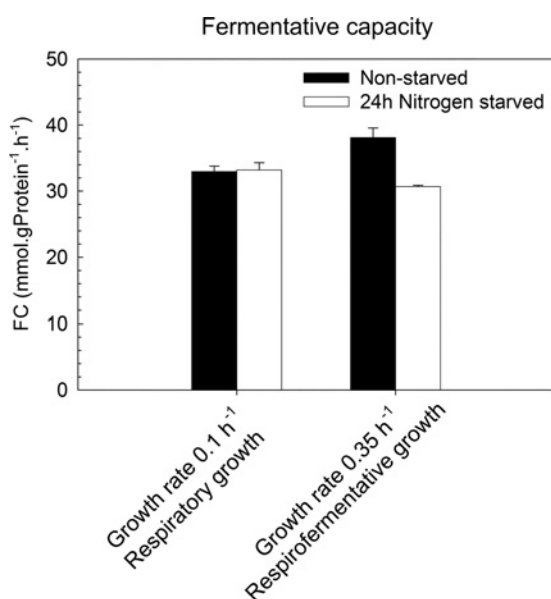


Figure 1 Stability of the fermentative capacity after 24 h of nitrogen starvation

Error bars represent SEM of at least three experiments on independent cultures. The data from the respirofermentative cultures were obtained from [10]

respiratory and respirofermentative metabolism at the two different growth rates (Table 1). Subsequently, the cells were starved for nitrogen in the presence of an excess of glucose. The addition of glucose served to prevent additional starvation for the carbon source. In previous research a control experiment was done in which the cells were shifted to glucose excess, but in the continued presence of nitrogen [10]. These experiments were carried out only for the cells grown at a growth rate of 0.35/h. Results showed that nitrogen starvation caused the decrease in fermentative capacity. However, the effect of nitrogen starvation may be counteracted by the addition of the extra glucose. The fermentative capacity, that is the ethanol flux under anaerobic conditions at glucose excess, was determined in an off-line assay, in starved as well as non-starved cells. To this end, cells were washed and transferred to an anaerobic vessel with fresh and complete medium with an excess amount of glucose (56 mM). This condition mimics the situation of baker's yeast in dough [11]. Apart from the ethanol flux also the fluxes of glucose, glycerol, acetate, succinate, pyruvate and trehalose were determined over a period of 30 min. The production fluxes of acetate, pyruvate and succinate were always below 1% of the rate of glucose consumption. The carbon consumed in the off-line assay matched the

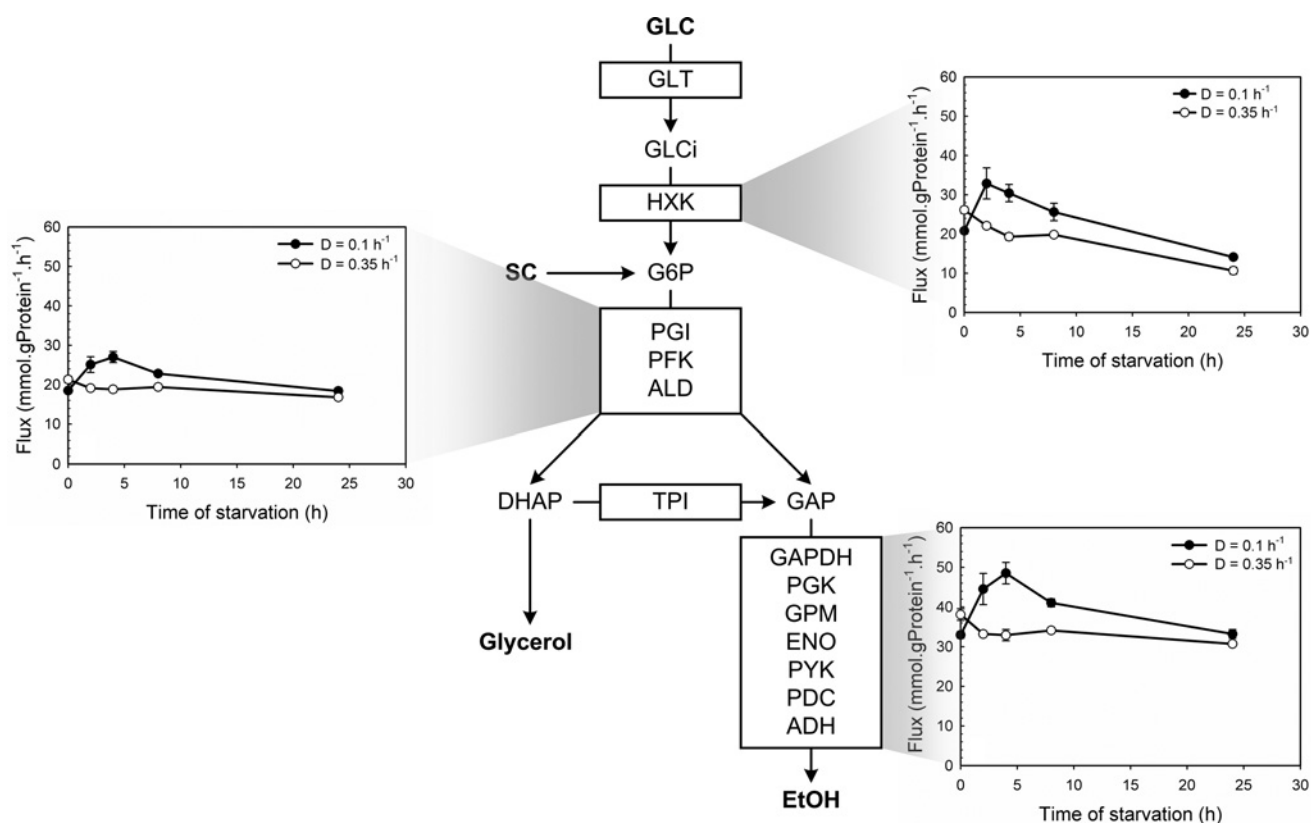


Figure 2 Fluxes through the glycolytic and fermentative pathways under anaerobic glucose-excess conditions

Fluxes were determined in an off-line fermentative-capacity assay at various time points during nitrogen starvation in cells from respiratory (closed circles, $D = 0.1/h$) and respirofermentative (open circles, $D = 0.35/h$) cultures. A simplified scheme of the glycolytic and fermentative pathways is shown in which the enzymes with the same flux are boxed. Measured fluxes are depicted in boldface letters and branching metabolites connect the boxes. Fluxes were calculated using the stoichiometry of the glycolytic and fermentative pathways (described in Material and Methods). In the graphs fluxes through glycolytic and fermentative pathways are plotted in time. Error bars represent SEM of at least three independent experiments carried out on different chemostat cultures. The data from the respirofermentative cultures ($D = 0.35/h$) were obtained from [10], except for the data at time point 8 h

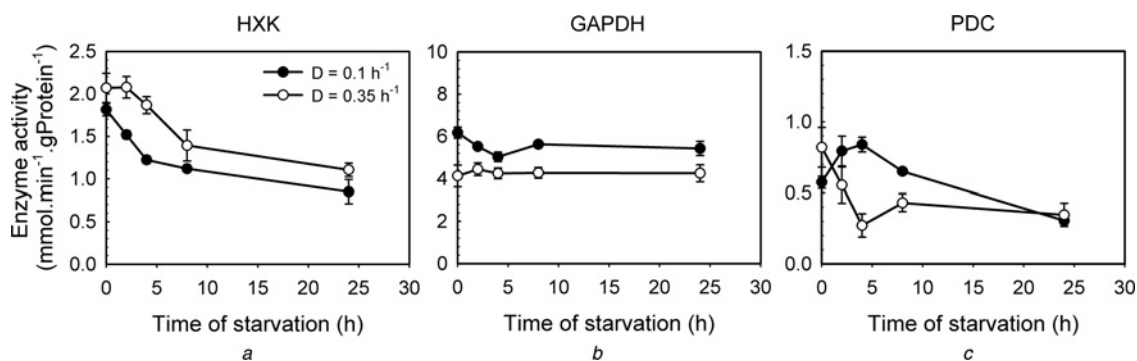


Figure 3 Enzyme capacities (V_{max}) during nitrogen starvation in cells from respiratory (closed circles, $D = 0.1/h$) or respirofermentative (open circles, $D = 0.35/h$) cultures

a HXK
b GAPDH
c PDC

Error bars represent the SEM of three independent experiments carried out on different chemostat cultures. The data from the respirofermentative cultures ($D = 0.35/h$) were obtained from [10], except for the data at time point 8 h

produced carbon within the experimental error for all time points, except for time point 2 h from the cells grown under respiratory conditions (see Table 2). In this particular case the carbon consumption was significantly higher than the carbon production. It is unlikely that the difference might be explained by the production of glycogen, since glycogen is usually consumed during glucose-excess conditions instead of produced. However, we have found substantial variation in the glucose-flux measurements for this time point, which we could not explain. Fig. 1 shows the fermentative capacity before and after 24 h of nitrogen starvation. In agreement with earlier results the fermentative capacity was lower in cells from respiratory cultures than in the cells from respirofermentative cultures [1]. However, after 24 h of starvation the fermentative capacity was more stable in cells from the respiratory cultures.

Fig. 2 shows how the fluxes measured in the fermentative-capacity assay for both respiratory ($D = 0.1/h$) and respirofermentative ($D = 0.35/h$) cultures developed in time during nitrogen starvation. The trends of the fluxes through upper and lower glycolysis were similar. In cells grown under respirofermentative conditions a 20% decrease in flux was observed during nitrogen starvation. In contrast, in the cells from respiratory cultures the fermentative capacity was increased by 45% during the first hours of nitrogen starvation and then decreased to initial levels. The increase and decrease of the fluxes compared to 0 h time point in the two experiments were significant (Student's t test, $P < 0.05$) for all time points, except for the 2 and 24 h time point in the respiratory experiment and the 2 h time point in the respirofermentative experiment.

3.2 Enzyme capacity

To investigate to what extent the changes in fluxes that occurred during nitrogen starvation were regulated by changes in the expression of the glycolytic and fermentative enzymes, we monitored their maximum activities (V_{max}) in

time. Fig. 3 shows three examples of enzyme capacity patterns observed in cells from respiratory and respirofermentative cultures. HXK (Fig. 3a) showed a gradual decrease of enzyme capacity in both experiments and similar patterns were observed for PGI, PFK, ALD and ADH. The capacity of GAPDH (Fig. 3b) did not change significantly in both experiments. A similar pattern was found for pyruvate kinase (PYK). However, the capacity of PYK was decreased significantly in the 2 and 4 h time points in the cells from the respirofermentative cultures (Student's t test, $P < 0.05$). The pattern of pyruvate decarboxylase (PDC) (Fig. 3c) mostly resembled that of the flux. Its capacity decreased in cells grown under respirofermentative conditions, whereas it first increased and then decreased in the cells from the respiratory cultures. A similar pattern was found for PGK, but the V_{max} of the latter recovered after an initial decrease in cells from the respirofermentative culture.

3.3 Time-dependent Regulation Analysis

To understand how the distribution of regulation between metabolism and gene expression differed between cells obtained from respiratory and respirofermentative cultures, time-dependent Regulation Analysis was applied to the data. Hierarchical (gene expression) and metabolic regulation coefficients were calculated relative to t_0 (just after the transfer of the cells to the nitrogen-free medium) by using the integrative form of time-dependent Regulation Analysis (Equations 1–2). Fig. 4 shows the hierarchical regulation coefficients of all the enzymes measured. Since after 24 h of nitrogen starvation, the fluxes of cells from respiratory cultures were back to their values at t_0 , the denominator of (1) became very small and no regulation coefficients could be computed reliably.

For nearly all enzymes the hierarchical regulation coefficients were higher in the cells from respirofermentative cultures than in the cells from respiratory cultures. This is even more

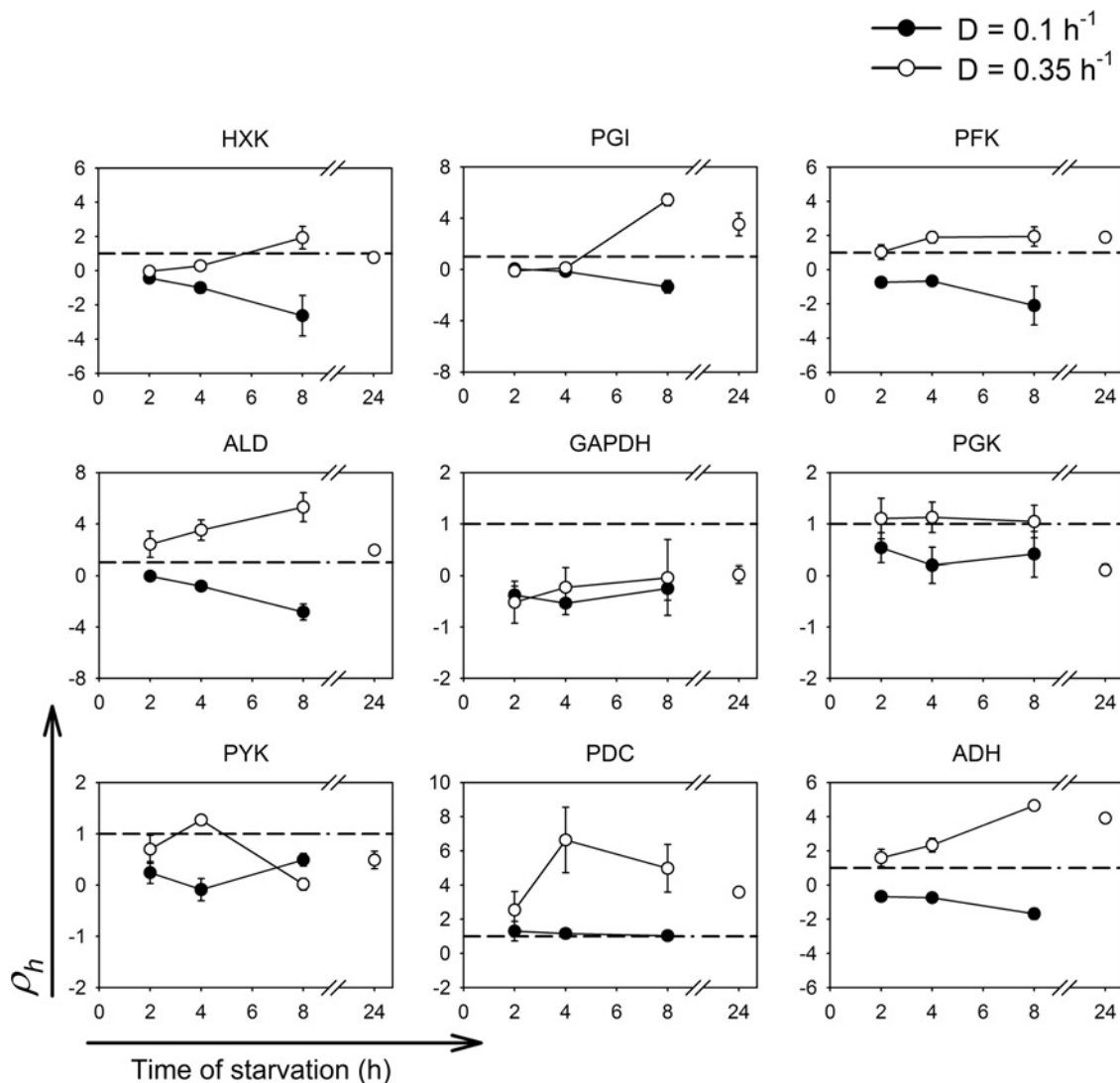


Figure 4 Hierarchical regulation coefficients of cells from respiratory (closed circles, $D = 0.1/h$) and respirofermentative (open circles, $D = 0.35/h$) cultures during nitrogen starvation

Error bars represent SEM of three independent experiments carried out on different chemostat cultures and were calculated as follows: averages and standard deviations (SD) were calculated separately for the numerator and the denominator of (3). Based on the SDs of the numerator and the denominator the SEM of ρ_h was computed. The dashed lines indicate a ρ_h of 1.0 and the dotted lines indicate a ρ_h of 0. The data from the respirofermentative cultures ($D = 0.35/h$) were obtained from [10], except for the data at time point 8 h

obvious in Fig. 5, in which we plotted the distribution of the regulation coefficients in two ways. In panel A the metabolic regulation coefficient is plotted against the hierarchical regulation coefficient. In this scatter plot we see a range, largely coinciding with cooperative regulation, in which the regulation coefficients of both experiments are overlapping. However, for the respirofermentative experiment we see that the regulation spreads out into the direction in which hierarchical regulation is more dominant, whereas in the respiratory experiment the regulation spreads out into the direction in which metabolic regulation is dominant. The same can be observed in panel B of Fig. 5, but then one can also distinguish in which direction the flux changes. In the cells from respirofermentative cultures the flux decreased and thus all the dots ended up left to the Y-axis. The opposite holds for the cells from respiratory cultures, where the flux

increased and thus nearly all dots ended up right to the Y-axis. One exception is the flux through hexokinase after 24 h of nitrogen starvation in cells from respiratory cultures. In this specific point the flux decreased compared to t_0 . Again both experiments had dots in the area of cooperative regulation whereas most other dots of the respirofermentative experiment were in the area where hierarchical regulation is dominant, whereas the remaining dots of the respiratory experiment were in the area where metabolic regulation is dominant.

3.4 Intracellular metabolite concentrations

Because in the cells grown under respiratory conditions the flux through glycolysis was predominantly regulated by metabolism, the next step was to study the changes in the

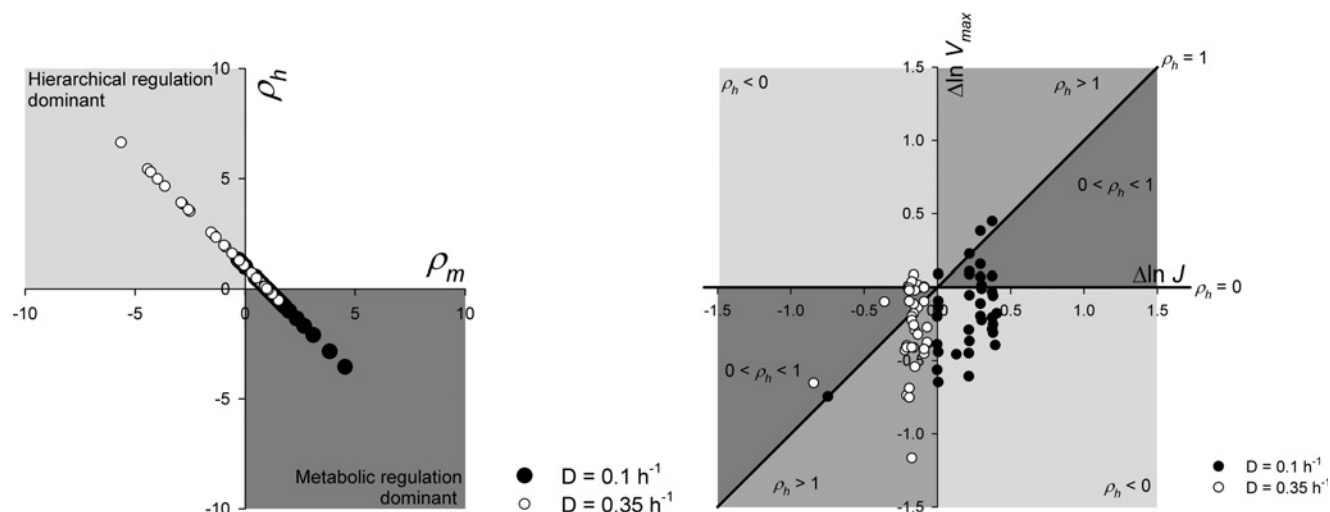


Figure 5 Distribution of the regulation coefficients

Left panel: scatter plot of the metabolic regulation coefficients against the hierarchical regulation coefficients. Right panel: scatter plot of the $\Delta \ln J$ against the $\Delta \ln V_{\max}$. The different categories are as follows, $\rho_h = 1$: purely hierarchical regulation, $\rho_h = 0$ purely metabolic regulation, $0 < \rho_h < 1$: cooperative regulation by changed V_{\max} and metabolism, $\rho_h > 1$: antagonistic regulation in the direction of V_{\max} , $\rho_h < 0$: antagonistic regulation in the direction of metabolism. The data from the respirofermentative cultures ($D = 0.35/h$) were obtained from [10], except for the data obtained at time point 8 h

intracellular concentrations of the metabolites. We have focused on the time points 0 and 4 h after the start of nitrogen starvation, since the difference in flux between both growth conditions was largest at these time points. Samples were taken at 15 min after addition of glucose in the fermentative-capacity assay. Fig. 6 shows the intracellular metabolite concentrations relative to total protein, of the glycolytic metabolites G6P, fructose-6-phosphate (F6P), fructose-1,6-bisphosphate (F1,6bP), 2-phosphoglycerate (2PGA) + 3-phosphoglycerate (3PGA), phosphoenolpyruvate (PEP) and pyruvate. The levels of these intermediates did not vary appreciably between the four different conditions. In all cases, the relatively high levels of F1,6bP and pyruvate and low levels of PEP and 2PGA + 3PGA are consistent with the characteristic pattern for conditions of high glycolytic flux [13, 20]. Furthermore, the levels of G6P, F1,6bP and pyruvate were significantly higher (Student's t test, $P < 0.05$) in the non-starved cells from the respirofermentative culture. Previous literature suggested that the intracellular concentrations of G6P and F1,6bP correlate positively with the flux [21]. This is not in agreement with our experiments, since the highest flux was measured in the 4 h nitrogen-starved cells from the respiratory culture.

In addition, the most important known allosteric regulators of glycolytic enzymes, trehalose-6-phosphate (T6P), citrate and fructose-2,6-bisphosphate (F2,6bP), were measured (Fig. 6). The changes in the regulators were much larger than those of the glycolytic intermediates, most noticeably between the non-starved and the 4 h nitrogen-starved cells. We investigated whether the pattern of the regulators by itself could explain the observed metabolic regulation. In the cells from the respiratory cultures the flux through HXK and PFK increased. Both

enzymes were then regulated negatively by gene expression so metabolic regulation should explain the drastic increase in the flux through these enzymes. A relief of inhibition of HXK by a strongly decreased level of the inhibitor T6P [22, 23] indeed works in this direction. However, the increase of the PFK inhibitor citrate [24] and the decrease of its activator F2,6bP [25, 26] work in the opposite direction. In the case of cells grown under respirofermentative conditions the metabolic regulation was much weaker. The decrease of the flux through HXK was then regulated cooperatively by metabolism and gene expression. The decreased level of T6P, however, would stimulate the enzyme and can therefore not explain the metabolic part of the regulation by itself. The flux through PFK decreased only slightly, whereas the V_{\max} showed a stronger decrease. Therefore stimulatory metabolic effects are expected. The increase of the activator F2,6bP fits in this picture, but the increase of the inhibitor citrate does not.

The levels of ATP, ADP and AMP were also measured in the same set of samples (Fig. 6). The total pool of adenine nucleotides is not constant. The largest absolute changes are observed for ATP, which correlates negatively with the flux through the pathway (cf. Fig. 2, time points 0 and 4 h). Such negative correlation between the ATP level and the flux was also found by Larsson *et al.* [27, 28]. The correlation could be a reflection of product inhibition of glycolysis, either directly at the level of the ATP producing enzymes PGK and PYK or via allosteric inhibition of glycolytic enzymes by ATP [29, 30].

4 Discussion

We investigated how the flux through glycolysis was regulated in time upon nitrogen starvation in cells with

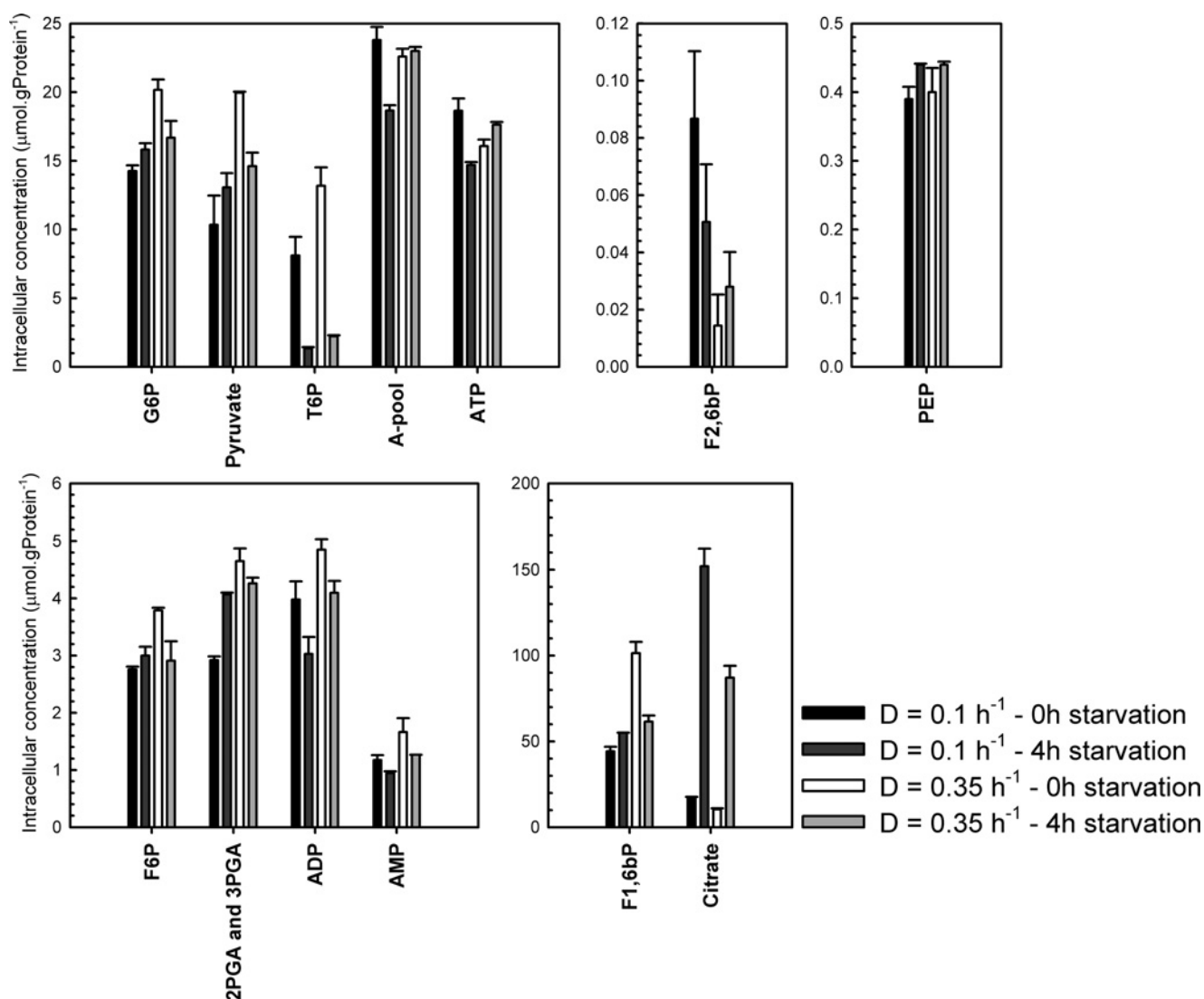


Figure 6 Intracellular metabolite levels

Error bars represent SDs of two independent experiments carried out on different chemostat cultures (each comprising duplicate samples, each analysed at least in duplicate)

different growth histories. In this study, cells from respiratory and respirofermentative cultures were subjected to nitrogen starvation. In accordance with earlier studies [1, 11] we observed that the fermentative capacity of cells grown under respiratory conditions was lower than that of cells from respirofermentative cultures. The former was, however, more stable upon prolonged exposure to the nitrogen starvation. The detailed time profiles revealed that the fermentative capacity even increased transiently in cells from respiratory cultures during the first 4 h of nitrogen starvation. In cells grown under respirofermentative conditions the fermentative capacity decreased from the onset of nitrogen starvation.

In both experiments diverse categories of regulation were found. However, in the cells grown under respiratory conditions regulation was dominated by metabolism, whereas in the cells grown under respirofermentative conditions hierarchical regulation was dominant. During

the transient increase of the fermentative capacity in the respiratory cells ρ_m was larger than ρ_h for all enzymes except for PDC. During the decrease of the fermentative capacity in the respirofermentative cells the ρ_h was rather larger than ρ_m for all enzymes except GAPDH and PYK. In the respirofermentative cells some (but not all) of the decrease of fermentative capacity can be attributed to breakdown of the glycolytic proteins during nitrogen starvation [31, 32]. Unlike Rossell *et al.* [5] we also observed a significant breakdown of the glycolytic proteins when the respiratory cells were subjected to nitrogen starvation. The transient increase of the fermentative capacity must therefore be attributed to a counteracting and dominant metabolic regulation.

The role of pyruvate decarboxylase is intriguing. Of all enzymes it was the only enzyme that showed a V_{\max} pattern similar to that of the fermentative capacity in both experiments. Accordingly, this enzyme was hierarchically

regulated under both conditions. Similar observations were made when the changes of fermentative capacity at different dilution rates in chemostats were studied [1]. It is tempting therefore to suggest that changes of the V_{\max} of pyruvate decarboxylase are the primary cause of changes in fermentative capacity. Flikweert *et al.* [33] showed that a reduction of PDC activity resulted in a reduced production of fermentation products. However, PDC overexpression did not result in a higher fermentative capacity [34], suggesting that other enzymes also need to be overexpressed to achieve a higher fermentative capacity. If also in our experiments the changes of the V_{\max} of pyruvate decarboxylase are not the sole cause of the changes of fermentative capacity, then the metabolic regulation of the other enzymes not only can be caused by changes inside glycolysis, but also must come from outside.

Since allosteric regulators, that is F2,6bP, T6P and citrate, may play an important role in the regulation of the flux [35], we hypothesised that a substantial part of the metabolic regulation would be due to changes in their intracellular levels. Therefore intracellular levels of the allosteric regulators, as well as of the glycolytic intermediates were determined under the conditions of the fermentative-capacity assay. The most substantial differences were indeed found in the levels of the allosteric regulators of the glycolytic enzymes, that is T6P, citrate and F2,6bP, whereas the levels of the glycolytic intermediates themselves did not change much. However, apart from the relief of inhibition of HXK by T6P in the cells grown under respiratory conditions, the changes in the allosteric regulators by themselves could not explain the metabolic regulation that was observed. This failure raises the possibilities that metabolite–enzyme interactions described *in vitro* may not give a complete picture of the *in vivo* situation and that additional regulators may exist which have yet to be identified. Also changes in the adenine nucleotides, notably ATP, were observed. ATP has both activating and inhibitory effects on different steps in glycolysis and therefore a quantitative kinetic model is required to predict the net effect of changes in ATP. In addition, the rate of each enzyme is determined by a number of concentrations of substrates, products and effectors simultaneously. An important step in explaining the changes in flux upon nitrogen starvation in cells from either respiratory or respirofermentative cultures will therefore be the implementation of the obtained data into a kinetic model of the pathway. As a starting point we use the glycolysis model of Teusink *et al.* [36]. It will be necessary to extend the model, to include all the known allosteric regulators.

In conclusion, the results obtained with time-dependent Regulation Analysis showed us how the regulation of the fermentative capacity during nitrogen starvation depends on the cell history. Our current work focuses (i) on the importance of protein degradation by explicit distinction of protein synthesis and degradation and (ii) on explaining the observed changes in flux by applying the model of Teusink *et al.* [36] to the case of nitrogen starvation.

5 Acknowledgment

This project was financially supported by the IOP Genomics program of Senter Novem. The work of B.M. Bakker and H.V. Westerhoff is further supported by STW, NCI-Kluyver Centre, NWO-SysMO and EU grants BioSim, NucSys and UniCellSys. The CEN.PK113-7D strain was kindly donated by P. Kötter, Euroscarf, Frankfurt.

This paper is an enhanced and expanded version of work originally presented at the 13th Workshop of the International Study Group for Systems Biology (ISGSB '08), held in Elsinore (Helsingør), Denmark in August 2008.

6 References

- [1] VAN HOEK P., VAN DIJKEN J.P., PRONK J.T.: 'Regulation of fermentative capacity and levels of glycolytic enzymes in chemostat cultures of *Saccharomyces cerevisiae*', *Enzyme Microb. Technol.*, 2000, **26**, (9–10), pp. 724–736
- [2] NILSSON A., NORBECK J., OELZ R., BLOMBERG A., GUSTAFSSON L.: 'Fermentative capacity after cold storage of baker's yeast is dependent on the initial physiological state but not correlated to the levels of glycolytic enzymes', *Int. J. Food Microbiol.*, 2001, **71**, (2–3), pp. 111–124
- [3] NILSSON A., PAHLMAN I.L., JOVALL P.A., BLOMBERG A., LARSSON C., GUSTAFSSON L.: 'The catabolic capacity of *Saccharomyces cerevisiae* is preserved to a higher extent during carbon compared to nitrogen starvation', *Yeast*, 2001, **18**, (15), pp. 1371–1381
- [4] DIDERICH J.A., RAAMSDONK L.M., KRUCKEBERG A.L., BERDEN J.A., VAN DAM K.: 'Physiological properties of *Saccharomyces cerevisiae* from which hexokinase II has been deleted', *Appl. Environ. Microbiol.*, 2001, **67**, (4), pp. 1587–1593
- [5] ROSSELL S., LINDENBERGH A., VAN DER WEIJDEN C.C., *ET AL.*: 'Mixed and diverse metabolic and gene-expression regulation of the glycolytic and fermentative pathways in response to a HXK2 deletion in *Saccharomyces cerevisiae*', *FEMS Yeast Res.*, 2008, **8**, (1), pp. 155–164
- [6] ROSSELL S., VAN DER WEIJDEN C.C., KRUCKEBERG A.L., BAKKER B.M., WESTERHOFF H.V.: 'Hierarchical and metabolic regulation of glucose influx in starved *Saccharomyces cerevisiae*', *FEMS Yeast Res.*, 2005, **5**, (6–7), pp. 611–619
- [7] TER KUILE B.H., WESTERHOFF H.V.: 'Transcriptome meets metabolome: hierarchical and metabolic regulation of the glycolytic pathway', *FEBS Lett.*, 2001, **500**, (3), pp. 169–171
- [8] BRUGGEMAN F.J., DE HAAN J., HARDIN H., *ET AL.*: 'Time-dependent hierarchical regulation analysis: deciphering cellular adaptation', *Syst. Biol. (Stevenage)*, 2006, **153**, (5), pp. 318–322

- [9] ROSSELL S., VAN DER WEIJDEN C.C., LINDENBERGH A., *ET AL.*: 'Unraveling the complexity of flux regulation: a new method demonstrated for nutrient starvation in *Saccharomyces cerevisiae*', *Proc. Natl. Acad. Sci. USA*, 2006, **103**, (7), pp. 2166–2171
- [10] VAN EUNEN K., BOUWMAN J., LINDENBERGH A., WESTERHOFF H.V., BAKKER B.M.: 'Time-dependent regulation analysis dissects shifts between metabolic and gene-expression regulation during nitrogen starvation in baker's yeast', *Febs J.*, 2009, **276**, (19), pp. 5521–5536
- [11] VAN HOEK P., VAN DIJKEN J.P., PRONK J.T.: 'Effect of specific growth rate on fermentative capacity of baker's yeast', *Appl. Environ. Microbiol.*, 1998, **64**, (11), pp. 4226–4233
- [12] VERDUYN C., POSTMA E., SCHEFFERS W.A., VAN DIJKEN J.P.: 'Effect of benzoic acid on metabolic fluxes in yeasts: a continuous-culture study on the regulation of respiration and alcoholic fermentation', *Yeast*, 1992, **8**, (7), pp. 501–517
- [13] CANELAS A.B., RAS C., TEN PIERICK A., VAN DAM J.C., HEIJNEN J.J., VAN GULIK W.M.: 'Leakage-free rapid quenching technique for yeast metabolomics', *Metabolomics*, 2008, **4**, (3), pp. 226–239
- [14] GONZALEZ B., FRANCOIS J., RENAUD M.: 'A rapid and reliable method for metabolite extraction in yeast using boiling buffered ethanol', *Yeast*, 1997, **13**, (14), pp. 1347–1355
- [15] LANGE H.C., EMAN M., VAN ZUIJLEN G., *ET AL.*: 'Improved rapid sampling for in vivo kinetics of intracellular metabolites in *Saccharomyces cerevisiae*', *Biotechnol. Bioeng.*, 2001, **75**, (4), pp. 406–415
- [16] MASHEGO M.R., WU L., VAN DAM J.C., *ET AL.*: 'MIRACLE: mass isotopomer ratio analysis of U-13C-labeled extracts. A new method for accurate quantification of changes in concentrations of intracellular metabolites', *Biotechnol. Bioeng.*, 2004, **85**, (6), pp. 620–628
- [17] VAN DAM J.C., EMAN M.R., FRANK J., LANGE H.C., VAN DEDEM G.W.K., HEIJNEN S.J.: 'Analysis of glycolytic intermediates in *Saccharomyces cerevisiae* using anion exchange chromatography and electrospray ionization with tandem mass spectrometric detection', *Anal. Chim. Acta*, 2002, **460**, (2), pp. 209–218
- [18] WU L., MASHEGO M.R., VAN DAM J.C., *ET AL.*: 'Quantitative analysis of the microbial metabolome by isotope dilution mass spectrometry using uniformly 13C-labeled cell extracts as internal standards', *Anal. Biochem.*, 2005, **336**, (2), pp. 164–171
- [19] SEIFAR R.M., RAS C., VAN DAM J.C., VAN GULIK W.M., HEIJNEN J.J., VAN WINDEN W.A.: 'Simultaneous quantification of free nucleotides in complex biological samples using ion pair reversed phase liquid chromatography isotope dilution tandem mass spectrometry', *Anal. Biochem.*, 2009, **388**, (2), pp. 213–219
- [20] VAN DEN BRINK J., CANELAS A.B., VAN GULIK W.M., *ET AL.*: 'Dynamics of glycolytic regulation during adaptation of *Saccharomyces cerevisiae* to fermentative metabolism', *Appl. Environ. Microbiol.*, 2008, **74**, (18), pp. 5710–5723
- [21] BOSCH D., JOHANSSON M., FERNDAL C., FRANZEN C.J., LARSSON C., GUSTAFSSON L.: 'Characterization of glucose transport mutants of *Saccharomyces cerevisiae* during a nutritional upshift reveals a correlation between metabolite levels and glycolytic flux', *FEMS Yeast Res.*, 2008, **8**, (1), pp. 10–25
- [22] EASTMOND P.J., GRAHAM I.A.: 'Trehalose metabolism: a regulatory role for trehalose-6-phosphate?', *Curr. Opin. Plant Biol.*, 2003, **6**, (3), pp. 231–235
- [23] BLAZQUEZ M.A., LAGUNAS R., GANCEDO C., GANCEDO J.M.: 'Trehalose-6-phosphate, a new regulator of yeast glycolysis that inhibits hexokinases', *FEBS Lett.*, 1993, **329**, (1–2), pp. 51–54
- [24] YOSHINO M., MURAKAMI K.: 'AMP deaminase as a control system of glycolysis in yeast. Mechanism of the inhibition of glycolysis by fatty acid and citrate', *J. Biol. Chem.*, 1982, **257**, (18), pp. 10644–10649
- [25] HERS H.G., VAN SCHAFTINGEN E.: 'Fructose 2,6-bisphosphate 2 years after its discovery', *Biochem. J.*, 1982, **206**, (1), pp. 1–12
- [26] OKAR D.A., LANGE A.J.: 'Fructose-2,6-bisphosphate and control of carbohydrate metabolism in eukaryotes', *Biofactors*, 1999, **10**, (1), pp. 1–14
- [27] LARSSON C., NILSSON A., BLOMBERG A., GUSTAFSSON L.: 'Glycolytic flux is conditionally correlated with ATP concentration in *Saccharomyces cerevisiae*: a chemostat study under carbon- or nitrogen-limiting conditions', *J. Bacteriol.*, 1997, **179**, (23), pp. 7243–7250
- [28] LARSSON C., PAHLMAN I.L., GUSTAFSSON L.: 'The importance of ATP as a regulator of glycolytic flux in *Saccharomyces cerevisiae*', *Yeast*, 2000, **16**, (9), pp. 797–809
- [29] KOPETZKI E., ENTIAN K.D.: 'Glucose repression and hexokinase isoenzymes in yeast. Isolation and characterization of a modified hexokinase PII isoenzyme', *Eur. J. Biochem.*, 1985, **146**, (3), pp. 657–662
- [30] REIBSTEIN D., DEN HOLLANDER J.A., PILKIS S.J., SHULMAN R.G.: 'Studies on the regulation of yeast phosphofructo-1-kinase: its role in aerobic and anaerobic glycolysis', *Biochemistry*, 1986, **25**, (1), pp. 219–227

- [31] KLIONSKY D.J.: 'Autophagy: from phenomenology to molecular understanding in less than a decade', *Nat. Rev. Mol. Cell Biol.*, 2007, **8**, (11), pp. 931–937
- [32] MIZUSHIMA N., KLIONSKY D.J.: 'Protein turnover via autophagy: implications for metabolism', *Annu. Rev. Nutr.*, 2007, **27**, pp. 19–40
- [33] FLIKWEERT M.T., KUYPER M., VAN MARIS A.J., KOTTER P., VAN DIJKEN J.P., PRONK J.T.: 'Steady-state and transient-state analysis of growth and metabolite production in a *Saccharomyces cerevisiae* strain with reduced pyruvate-decarboxylase activity', *Biotechnol. Bioeng.*, 1999, **66**, (1), pp. 42–50
- [34] VAN HOEK P., FLIKWEERT M.T., VAN DER AART Q.J., STEENSMA H.Y., VAN DIJKEN J.P., PRONK J.T.: 'Effects of pyruvate decarboxylase overproduction on flux distribution at the pyruvate branch point in *Saccharomyces cerevisiae*', *Appl. Environ. Microbiol.*, 1998, **64**, (6), pp. 2133–2140
- [35] GONCALVES P., PLANTA R.J.: 'Starting up yeast glycolysis', *Trends Microbiol.*, 1998, **6**, (8), pp. 314–319
- [36] TEUSINK B., PASSARGE J., REIJENGA C.A., ET AL.: 'Can yeast glycolysis be understood in terms of in vitro kinetics of the constituent enzymes? Testing biochemistry', *Eur. J. Biochem.*, 2000, **267**, (17), pp. 5313–5329